Preparation of silicon-based nanowires through high-temperature annealing

Shuang Xi*, Shuangshuang Zuo, Ying Liu, Yinlong Zhu, Yutu Yang, Binli Gou

School of Mechanical and Electronical Engineering, Nanjing Forestry University, Nanjing 210037, China

shuangxi@hust.edu.cn

ABSTRACT. *This paper explores the effects of process parameters on the structure and morphology of silicon-based nanowires. Specifically, the substrate of silicon was annealed at high temperature or with a metal catalyst, such that numerous silicon-based nanowires were grown on the silicon wafer. Through the adjustment of process parameters, SiO_2 nanowires, Si_3N_4 nanowires and SiO_xN_y nanowires were produced with different morphologies. The process parameters that affect the final structure were determined as the carrier gas for annealing, the type of metal catalyst and the substrate surface. After that, the morphology of the nanowires was characterized by scanning electron microscopy (SEM), the composition of the nanowires was tested by energy dispersive X-ray spectroscopy (EDS), and the relationship between the microstructure of the nanowires and various parameters was analyzed by transmission electron microscopy (TEM). The results show that the Si_3N_4 nanowires and SiO_xN_y nanowires are single crystals requiring harsh preparing processes, while SiO_2 nanowires were amorphous and have low requirements on the growth environment. In addition, the optical properties of SiO_2 nanowire film and SiO_xN_y nanowire film were characterized, proving their ultra-bright whiteness. The research findings lay the theoretical basis for the controlled growth of silicon-based nanowires, and provide a simple and efficient method for batch growth of nanowires.*

RÉSUMÉ. *Cet article explore les effets des paramètres de processus sur la structure et la morphologie des nanofils en silicium. Plus précisément, le substrat de silicium a été recuit à haute température ou avec un catalyseur métallique, de sorte que de nombreux nanofils en silicium ont été développés sur la plaquettes de silicium. Grâce à l'ajustement des paramètres de processus, des nanofils de SiO_2, de Si_3N_4 et de SiOxNy ont été produits avec différentes morphologies. Les paramètres du procédé qui affectent la structure finale ont été déterminés en tant que gaz vecteur du recuit, type de catalyseur métallique et surface du substrat. Après cela, la morphologie des nanofils a été caractérisée par microscopie électronique à balayage (MEB en anglais), la composition des nanofils a été testée par l'analyse dispersive en énergie (EDS en anglais) et la relation entre la microstructure des nanofils et divers paramètres a été analysée par la microscopie électronique en transmission (MET en anglais). Les résultats montrent que les nanofils Si_3N_4 et les nanofils SiOxNy sont des monocristaux nécessitant un processus de préparation rigoureux, tandis que les nanofils SiO_2 sont amorphes et ont de faibles exigences en matière de croissance. De plus, les propriétés optiques des films de*

nanofils de SiO_2 et de SiOxNy ont été caractérisées, prouvant leur blancheur ultra-brillante. Les résultats de la recherche jettent les bases théoriques de la croissance contrôlée des nanofils en silicium et constituent une méthode simple et efficace pour la croissance par lots de nanofils.

KEYWORDS: silicon-based nanowires, high-temperature annealing, morphology, microstructure.

MOTS-CLÉS: nanofils en silicium, recuit à haute temperature, morphologie, microstructure.

DOI:10.3166/ACSM.42.149-158 © 2018 Lavoisier

1. Introduction

As an important semiconductor material, silicon plays an important role in the field of microelectronics. However, the application of bulk silicon in optoelectronic devices is very limited, because of the low luminous efficiency of the material. The low efficiency is attributable to the narrow forbidden band (Eg =1.17eV at T=0K and 1.14eV at T=300K) resulted from the indirect band gap of bulk silicon (Green, 2005; Kichou *et al.*, 2016; Meillaud *et al.*, 2015). Recent studies show that low-dimensional nano-silicon has completely different optical and electrical effects from bulk silicon, due to quantum confinement and Coulomb blockade. Under these effects, nano-silicon has been widely applied in such low-energy optoelectronic devices like bio/chemical sensors, high-speed field-effect tubes, and optoelectronics (Han and Chen, 2010; Cui *et al.*, 2003; Ueda *et al.*, 2015).

The unique properties of nano-silicon have attracted wide attention in the scientific community. So far, silicon-based nanowires of varied electrical, optical and mechanical properties have been prepared by different methods. For instance, SiO_2 nanowires are essential to near-field optical microscopy, low-dimensional waveguide and the connection of integrated optical devices, thanks to its good photoluminescence effect and waveguide effect (Loget and Corn, 2014; Colombelli *et al.*, 2016). With continuously adjustable light and electrical properties (e.g. the refractive index increased from 1.45 to 2.00 and the dielectric constant increased from 3.8 to 7.8 with the growth in the Y/X ratio), SiO_xN_y nanowires have been extensively used in optical fibers and waveguide devices (Zheng *et al.*, 2009; Xi *et al.*, 2013). Si_3N_4 nanowires enjoy excellent thermal performance in thermal shock resistance, oxidation resistance, high-temperature resistance and chemical stability (Zhang *et al.*, 2012).

The existing preparation methods for silicon-based nanowires include laser ablation, sol-gel method, thermal evaporation and chemical vapor deposition (Peled *et al.*, 2015; Seo *et al.*, 2015; Su *et al.*, 2014; Liu *et al.*, 2011; Yu *et al.*, 2016). In this paper, the chemical vapor deposition is coupled with high-temperature annealing to prepare numerous silicon-based nanowires on silicon wafers. Through the adjustment of process parameters, SiO_2 nanowires, Si_3N_4 nanowires and SiO_xN_y nanowires were produced with different morphologies. The author systematically explored the effects of the substrate surface, the carrier gas for annealing and the type of metal catalyst on the formation of nanowires. The various silicon-based nanowires, obtained through reasonably designed experiments, were subjected to

structural and morphological characterization by electron microscopy, and the analysis on optical properties.

2. Experiment

2.1. Instruments and reagents

The reagents, including acetone, concentrated sulfuric acid and hydrogen peroxide, are of chemical pure grade. The OTF-1200X quartz tube furnace for annealing was purchased from Hefei Kejing Material Technology Co., Ltd. The JEOL JSM-6610 scanning electron microscope (SEM) is equipped with an energy spectrometer (EDX). FEI Tecnai 12 transmission electron microscope (TEM) is from Thermo Fisher Scientific.

2.2. Experimental process

2.2.1. Preparation of nanowires without metal catalysts

A silicon wafer (single side polished) with 5nm natural oxide layer [100] was placed in acetone for 10min ultrasonic shaking, and then relocated to the SPM solution (concentrated sulfuric acid: hydrogen peroxide = 2:1) for 10min heating at 110℃. After that, the silicon wafer was rinsed with deionized water and blew dry by a nitrogen gun. The cleaned silicon wafer was placed in a quartz boat and relocated into a tube furnace. In the tube furnace, the silicon wafer could be placed with the polished side up or the unpolished side up. Next, the tube furnace was vacuumed, and the silicon wafer was heated up to 1,200℃ at 15℃/min in the atmosphere of Ar or N_2. The temperature was held for 2h before the silicon wafer was cooled naturally to room temperature.

2.2.2. Preparation of nanowires with metal catalysts

The silicon wafer and its cleaning procedure are the same as above. After cleaning, the silicon wafer was coated with a layer of metal film by magnetron sputtering. Two 99.9% pure metal targets, namely Cu and Ni, were used in the sputtering process. Next, the metal coated silicon wafer was placed in a quartz boat and relocated into a tube furnace. Then, the tube furnace was vacuumed, and the silicon wafer was heated up to 1,200℃ at 15℃/min in N_2 atmosphere. The temperature was held for 2h before the silicon wafer was cooled naturally under the N_2 atmosphere to room temperature.

2.2.3. Structure and performance characterization

The morphology of the silicon-based nanowires was investigated by field emission SEM. The composition of the nanowires was analyzed by the EDX on the SEM. The prepared nanowires were placed in ethanol for 30min ultrasonic shaking by an ultrasonic cleaner. Then, the uniformly dispersed solution was added dropwise

to the micro-grid. After drying, the microstructure of the nanowires was characterized by the TEM.

3. Results and discussion

Five experiments were designed with different process parameters: (1) no catalyst was used, N_2 was taken as the carrier gas, and the silicon wafer was placed with the polished side up; (2) no catalyst was used, N_2 was taken as the carrier gas, and the silicon wafer was placed with the unpolished side up; (3) no catalyst was used, Ar was taken as the carrier gas, and the silicon wafer was placed with the polished side up; (4) Ni was used as the catalyst, Ar was taken as the carrier gas, and the silicon wafer was placed with the polished side up; (5) Cu was used as the catalyst, N_2 was taken as the carrier gas, and the silicon wafer was placed with the polished side up. For simplicity, the samples obtained from the five experiments are denoted as sample (1), sample (2), sample (3), sample (4), and sample (5), respectively.

3.1. Morphology and structural characterization

Figure 1(a) is an SEM image of sample (1), in which the inset shows the EDX spectrum. The SEM image was blurry because of the fluffy and disordered growth of the nanowires.

In general, the nanowires were relatively long, reaching the length of several tens of micrometers or even hundreds of micrometers. The compositions were Si, O and N, that is, the nanowires in sample (1) are SiO_xN_y nanowires. More details of the microstructure were obtained by the TEM. As shown in Figure 1(b), the nanowires were smooth and straight, with a uniform diameter of 100nm. The light and dark stripes on the TEM image indicate the crystallinity of the nanowires. The inlet of Figure 1(b) presents the selected area electron diffraction (SAED) pattern, which proves the single-crystal structure of the nanowires.

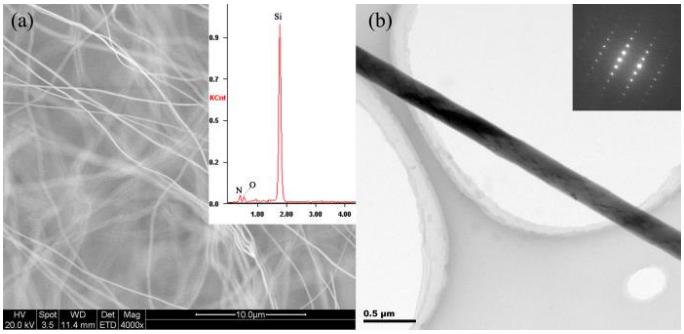

Figure 1. (a) SEM image of sample (1) (inlet: EDX spectrum); (b) TEM image of sample (1) (inlet: SAED pattern)

The characterization results of sample (2) are illustrated in Figure 2. It can be seen from the SEM image (Figure 2(a)) that the nanowires of sample (2) were not uniform in diameter. Some of them were thicker than the others. As shown in TEM pattern (Figure 2(b)), the thick ones could reach 300nm in diameter, much thicker than the nanowires in sample (1). A possible reason is that the unpolished side of the silicon wafer is much rougher than the polished side. That is why the nanowires had uneven sizes during nucleation and grown into different thicknesses. The EDX energy spectrum shows that the nanowires are SiO_2 nanowires, while the SAED results prove the amorphous structure of the nanowires.

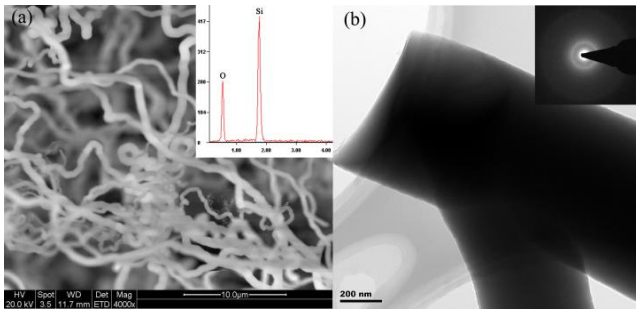

Figure 2. (a) SEM image of sample (2) (inlet: EDX spectrum); (b) TEM image of sample (2) (inlet: SAED pattern)

For sample (3), the carrier gas for high-temperature annealing was replaced by Ar. The morphology of this sample is shown in Figure 3 below. Compared to those in samples (1) and (2), the nanowires in sample (3) relatively curved amorphous SiO_2 nanowires with a diameter of 150~200nm.

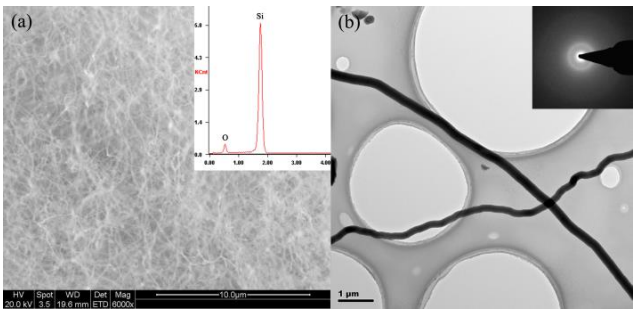

Figure 3. (a) SEM image of sample (3) (inlet: EDX spectrum); (b) TEM image of sample (3) (inlet: SAED pattern)

During the growth of nanowires, the addition of metal catalyst can promote nucleation and accelerate the growth rate. Taking Ni as the catalyst, the sample (4)

obtained after high-temperature annealing is displayed in Figure 4. As shown in the SEM image (Figure 4(a)), the nanowires grew straightly with metal particles on the top, revealing that the growth obeys the typical volatile-liquid-solid (VLS) mechanism. The EDX pattern shows that the nanowires were composed of Si and N. Considering the TEM and SAED in Figure 4(b), the nanowires were determined as single-crystal Si_3N_4 nanowires.

The morphology and structure of the nanowires obtained with Cu as the catalyst are given in Figure 5. It can be seen that the nanowires in sample (5) were mostly spiral in shape and short in length, and were amorphous SiO_2 nanowires. The comparison between sample (5) and sample (4) shows that different catalysts can produce nanowires with different compositions and structures. This means catalyst plays a very important role in the growth of nanowires.

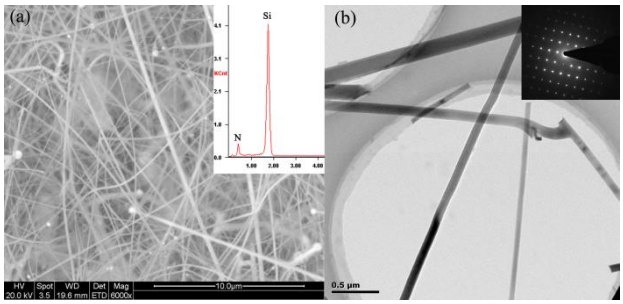

Figure 4. (a) SEM image of sample (4) (inlet: EDX spectrum); (b) TEM image of sample (4) (inlet: SAED pattern)

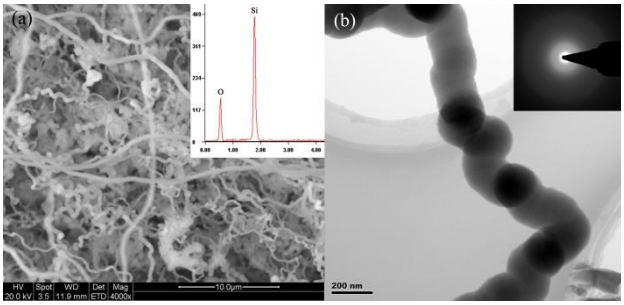

Figure 5. (a) SEM image of sample (5) (inlet: EDX spectrum); (b) TEM image of sample (5) (inlet: SAED pattern)

The silicon wafer was the sole source of Si in our research, as no other Si-containing materials were involved. For samples (1), (2) and (3), no liquid phase was generated during the growth of the nanowires, because no catalyst was introduced into the reaction and the melting point of Si was 1,414 ° C. Therefore, the

volatile-solid (VS) mechanism is the most possible growth mechanism of the three types of nanowires.

Under high temperature, the Si in the silicon wafer reacted with the SiO_2 in the surface oxide layer, forming SiO_x vapor. In experiment (1), Si-O-N nanoclusters were produced through the reaction between the SiO_x vapor and the carrier gas N_2. With the continuous supply of reactant gases, a 1D nanowire structure was developed through the continuous accumulation of SiO_xN_y.

In experiments (2) and (3), N_2 did not participate in the reactions. At above 1,200°C, SiO_2 came into being through the atomic recombination or oxidation of SiO_x. With the elapse of time, the concentration of SiO_2 molecules continued to increase until precipitation, which caused the growth of SiO_2 nanowires.

For samples (4) and (5), a metal catalyst was introduced into the reactions. Under high temperature, the metal film was melted into small droplets, which is conducive to nanowire nucleation. Therefore, the nanowire growth obeys the typical VLS mechanism.

In experiment (4), the SiO_x vapor diffused to the surface of metal Ni droplets, and fused with the latter into Ni-Si alloy. After that, the alloy reacted with the carrier gas N_2, forming Ni-Si-N alloy. With the continuous supply of SiO_x and N_2, the solid silicon nitride precipitated from the supersaturated melt, and eventually grew into Si_3N_4 nanowires.

In experiment (5), the Si in the silicon wafer reacted with the SiO_2 in the surface oxide layer, forming SiO_x vapor. With the elapse of the time, the SiO_x vapor continued to accumulate and diffused to the surface of metal droplets, creating Cu-Si alloy. As the SiO_x gas increased to saturation, the alloy finally precipitated and served as nuclei of crystallization. Thanks to the unceasing supply of Si and O, SiO_2 deposited on the nuclei continuously to form 1D nanowires.

Out of the five experiments, only experiments (1) and (4) produced single-crystal nanowires. The carrier gas N_2 participated in the reactions of both experiments, but not in those of the other three experiments. In the other three experiments, the nanowires are all amorphous SiO_2 nanowires. These phenomena indicate that single-crystal nanowires require harsh growth conditions like substrate, catalyst and ambient atmosphere, while amorphous SiO_2 nanowires have low requirements on the growth environment and are easier to prepare.

3.2. Optical performance characterization

In samples (1) and (5), the nanowire formation rates were high, and complete nanowire films were formed easily. Visual inspection shows that the films of the two samples were bright white in color, a sign of good optical reflection properties. To accurately characterize the optical properties, the reflectance of the two samples in the 350~800nm wavelength was tested using an ultraviolet–visible (UV-Vis) spectrophotometer. As shown in Figure 6(a), the reflectance of SiO_2 nanowire film was above 68% across the whole test range and peaked at 80%. The high reflectivity

in the visible light range gives the sample a super bright white color. For the SiO_xN_y nanowire film, the reflectance was maintained above 57% across the test band, reaching a maximum of 72% at 400nm. The prepared nanowire films have excellent reflection performance, especially in the ultraviolet band, which promises a good application potential in UV illumination devices.

To evaluate the chromaticity of the nanowire films, the coordinates (x, y) of the samples were determined against the CIE standard chromaticity diagram. As shown in Figure 6(b), the chromaticity coordinates of the SiO_xN_y nanowire film were (0.30, 0.34), and those of the SiO_2 nanowire film were (0.32, 0.32), both of which were extremely close to the coordinates of the white point (0.33, 0.33). This means the two nanowires are both brightly white and suitable for application in energy-saving building materials, white LEDs and white coatings.

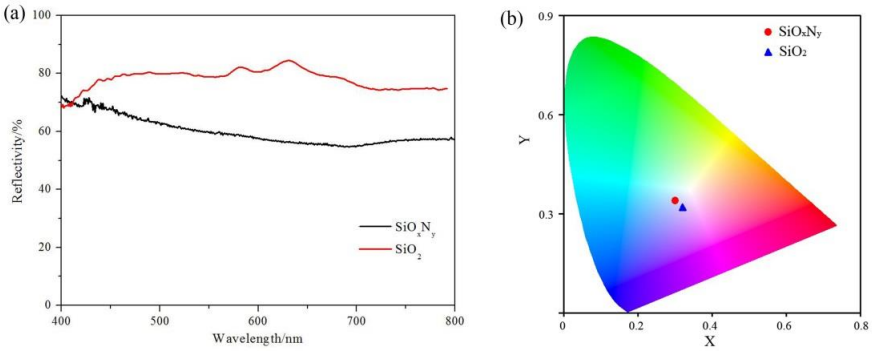

(a) Reflectance curves (b) CIE chromaticity diagram

Figure 6. Optical properties of samples (1) and (5)

4. Conclusions

Through high-temperature annealing, numerous silicon-based nanowires were prepared, including SiO_2 nanowires, Si_3N_4 nanowires and SiO_xN_y nanowires. The growth of these nanowires follows either the VS mechanism or the VLS mechanism. The experimental results show that single-crystal Si_3N_4 nanowires or SiO_xN_y nanowires were produced only when the silicon wafer was placed with the polished side up and the carrier gas was N_2; amorphous SiO_2 nanowires were the only product when the silicon wafer was placed with the unpolished side up, the carrier gas was replaced with another gas, and Cu was added as the catalyst. These phenomena indicate that single-crystal nanowires require harsh growth conditions like substrate, catalyst and ambient atmosphere. Next, the high reflectivity and ultra-bright white feature of SiO_2 nanowire film and SiO_xN_y nanowire film were verified through the characterization of optical performance, revealing the huge potential of these films in white light applications. The research findings lay a solid basis for the preparation of silicon-based nanowires of specific composition and structure.

Acknowledgement

This work is financially supported by Natural Science Foundation of Jiangsu Province (BK20160934).

References

Colombelli A., Manera M. G., Taurino A., Catalano M., Convertino A., Rella R. (2016). Au nanoparticles decoration of silica nanowires for improved optical bio-sensing. *Sensors and Actuators B-Chemical*, Vol. 226, pp. 589-597. https://doi.org/10.1016/j.snb.2015.11.075

Cui Y., Zhong Z., Wang D., Wang W. U., Lieber C. M. (2003). High performance silicon nanowire field effect transistors. *Nano letters*, Vol. 3, No. 2, pp. 149-152. https://doi.org/10.1021/nl025875l

Green M. A. (2005). Silicon photovoltaic modules: a brief history of the first 50 years. *Progress in Photovoltaics: Research and applications*, Vol. 13, No. 5, pp. 447-455. https://doi.org/10.1002/pip.612

Han S. E., Chen G. (2010). Optical absorption enhancement in silicon nanohole arrays for solar photovoltaics. *Nano Letters*, Vol. 10, No. 3, pp. 1012-1015. https://doi.org/10.1021/nl904187m

Kichou S., Abaslioglu E., Silvestre S., Nofuentes G., Torres-Ramirez M., Chouder A. (2016). Study of degradation and evaluation of model parameters of micromorph silicon photovoltaic modules under outdoor long term exposure in Jaén, Spain. *Energy Conversion and Management*, Vol. 120, pp. 109-119. https://doi.org/10.1016/j.enconman.2016.04.093

Liu D., Shi T. L., Tang Z. R., Zhang L., Xi S., Li X. P., Lai W. X. (2011). Carbonization-assisted integration of silica nanowires to photoresist-derived three-dimensional carbon microelectrode arrays. *Nanotechnology*, Vol. 22, No. 46, https://doi.org/10.1088/0957-4484/22/46/465601

Loget G., Corn R. M. (2014). Silica nanowire arrays for diffraction-based bioaffinity sensing. *Chemistry-A European Journal*, Vol. 20, No. 34, pp. 10802-10810. https://doi.org/10.1002/chem.201304800

Meillaud F., Boccard M., Bugnon G., Despeisse M., Hänni S., Haug F. J., Persoz J., Schüttauf J. W., Stuckelberger M., Ballif C. (2015). Recent advances and remaining challenges in thin-film silicon photovoltaic technology. *Materials Today*, Vol. 18, No. 7, pp. 378-384. https://doi.org/10.1016/j.mattod.2015.03.002

Peled E., Patolsky F., Golodnitsky D., Freedman K., Davidi G., Schneier D. (2015). Tissue-like silicon nanowires-based three-dimensional anodes for high-capacity lithium ion batteries. *Nano Letters*, Vol. 15, No. 6, pp. 3907-3916. https://doi.org/10.1021/acs.nanolett.5b00744

Seo K., Wober M., Steinvurzel P., Schonbrun E., Dan Y., Ellenbogen T., Crozier K. B. (2015). Multicolored vertical silicon nanowires. *Nano Letters*, Vol. 11, No. 4, pp. 1851-1856. https://doi.org/10.1021/nl200201b

Su X., Wu Q., Li J., Xiao X., Lott A., Lu W., Sheldon B. W., Wu J. (2014). Silicon-based nanomaterials for lithium-ion batteries: A review. *Advanced Energy Materials*, Vol. 4, No.

1. https://doi.org/10.1002/aenm.201300882

Ueda A., Luisier M., Sano N. (2015). Enhanced impurity-limited mobility in ultra-scaled Si nanowire junctionless field-effect transistors. *Applied Physics Letters*, Vol. 107, No. 25. https://doi.org/10.1063/1.4937901

Xi S., Shi T., Zhang L., Liu D., Lai W., Tang Z. (2013). Highly visible-light reflective SiO_xN_y nanowires for bright-white reflector applications. *Thin Solid Films*, Vol. 529, pp. 115-118. https://doi.org/10.1016/j.tsf.2012.07.077

Yu P., Wu J., Liu S., Xiong J., Jagadish C., Wang Z. M. (2016). Design and fabrication of silicon nanowires towards efficient solar cells. *Nano Today*, Vol. 11, No. 6, pp. 704-737. https://doi.org/10.1016/j.nantod.2016.10.001

Zhang L., Shi T., Tang Z., Liu D., Xi S. (2012). Stress-driven and carbon-assisted growth of SiO_xN_y nanowires on photoresist-derived carbon microelectrode. *Journal of Microelectromechanical Systems*, Vol. 21, No. 6, pp. 1445-1451. https://doi.org/10.1109/jmems.2012.2211570

Zheng L. R., Huang B. B., Wei J. Y. (2009). Carbon Assisted CVD synthesis of SiO_x nanowires and their optical property. *Chemical Journal of Chinese Universities*, Vol. 30, No. 2, pp. 250-254. https://doi.org/10.1115/MNHMT2009-18287